Convective oscillations in a laboratory model

Lianke te Raa

Abstract

A laboratory experiment has been conducted in which a small basin was heated from below. This basin was connected to a large reservoir that was filled with a layer of salt water at the bottom and fresh water above it, by tubes at the top, the middle and the bottom. It was shown that different flow regimes exist in this experiment. For low forcing temperatures, self-sustained oscillations occur, whereas the system reaches a steady state with deep convection for higher forcing temperatures. During an oscillation a shallow convecting layer of salty water at the bottom of the basin grows and entrains fresh water, until the water column becomes unstable and deep convection can occur. Inflow of salty water through the bottom tube stops the deep convection and the cycle starts again. In a configuration in which the top and middle tubes had smaller diameters, no oscillations were found. Instead, a regime with steady shallow convection states and a regime with steady deep convection states were found.

1 Introduction

An important part of the ocean's thermohaline circulation is the formation of deep water at high latitudes. Locations of deep convection are confined to certain specific areas in the North Atlantic Ocean and near Antarctica, including the Greenland-Norwegian Sea, the Labrador Sea, the Weddell Sea and the Ross Sea [1]. There are two types of deep convection in the ocean. One is convection near an ocean boundary, where dense water reaches the bottom of the ocean by descending a continental slope. The second process is called open-ocean convection and involves sinking of water in narrow area's far away from land. In both cases deep convection is a very complicated process, but general features of the polar oceans that are important are the intense surface cooling and the very fresh surface water [2]. In order to get deep convection an increase in salinity of the surface water is therefore needed, for instance due to brine rejection or mixing with a saltier water mass [3]. Due to these and other conditions, the areas in which deep-water formation occurs are not only small compared to the total area of the ocean, but the deep convection required for producing dense bottom water does also not occur every winter.

A good way to gain more understanding of complex processes as deep convection is the use of simple models. Recently, Whitehead [4] analyzed a simplified box model consisting of a small basin that is cooled from above and that is connected via three tubes to a large isothermal basin with a fresh surface layer. This is a very schematic model of the situation in the Arctic Ocean. For small cooling rates this model was shown to exhibit a steady state with shallow convection, whereas for strong cooling a state with deep convection occurred.

In the shallow state fresh and warm water enters the small basin via the upper tube, is cooled and convects downward and leaves through the middle tube. Or, if the cooling is stronger, water comes in through the upper tube and leaves via both the middle and the bottom tube. In the deep convection state the warm and fresh water enters the small basin through the upper tube, but there is also inflow of warm and salty water through the middle tube, whereas cold water leaves the small basin through the bottom tube.

If the cooling rate depends on temperature via a relaxation condition, this model was shown to exhibit multiple equilibria: both the shallow and the deep convection state could exist for the same forcing temperature [4]. In this case, sudden rapid transitions between both states can occur for only very slight changes in forcing temperature. Although obviously these results cannot be simply extended to the real ocean, these model results might still have important implications for the ocean. Periods of deep water formation might be followed by periods of shallow convection in which only intermediate water is formed if forcing conditions change slightly.

The original goal for this summer project was to investigate if the multiple equilibria predicted by the theoretical box model can also be found in the laboratory. However, the project evolved in a different direction, so that finally it turned out to be an exploration of the behavior of the flow in the laboratory version of this convective model. The laboratory model was turned upside-down with respect to the case of the Arctic Ocean (heating at the bottom and a layer of salty water at the bottom of the large basin) for practical reasons.

The theoretical model of Whitehead [4] is presented in section 2 of this report. This section closely follows his derivation, but describes the situation for the case with heating at the bottom instead of cooling at the top. The experimental apparatus and method are described in section 3.1 and the results follow in section 3.2 and 3.3. In section 4 the experimental results are compared to the box model theory and a discussion and the conclusions are given in section 5.

2 Theory

A small basin with two layers of water in a field of gravity is heated from below. This small basin is connected to a large basin, which is called the reservoir, with three tubes, one at the surface, one at mid-depth ($D/2$) and one at a depth D (Fig. 1). The reservoir contains a layer of salty water of salinity S_0 of constant thickness d with fresh water above it. Both layers have temperature T_0 (room temperature). The reservoir is taken to be so large and so well mixed that d, T_0 and S_0 remain fixed, irrespective of the flow into and out of the tubes.

In the small basin a convecting layer of thickness δ of water with temperature $T_0 + T$ and salinity S will develop, where δ, T and S still have to be determined. This layer is assumed to be well mixed, as it is heated from below, and its thickness will grow with increasing heating rate. Heat losses are neglected and it is assumed that there is no mixing of heat and salt across the interface between the warm and salty, convecting layer and the non-convecting layer of cold and fresh water above it.

The flow through the tubes is determined by the pressure difference between the two ends of the tubes and depends therefore on temperature and salinity in both the small basin and the reservoir. We assume that there is a steady-state relation between the flow through

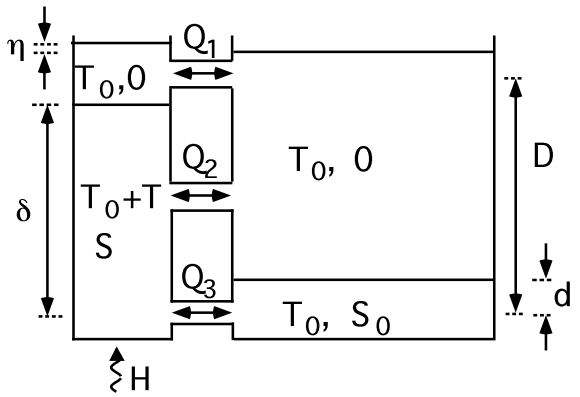

Figure 1: Sketch of the model configuration. The reservoir contains a layer of fresh water with temperature T_0 and zero salinity overlying a layer of salty water with the same temperature and salinity S_0. The temperatures and salinities in this basin remain constant. The temperature T and salinity S in the convecting layer in the small basin are determined by the flow rates Q_1, Q_2 and Q_3 and the heating rate H.

a tube and the pressure difference between the small basin and the reservoir at the height of that tube. The volume flux through tube i is denoted by Q_i, where $i = 1, 2, 3$ denotes top, middle and bottom tube, respectively and can then be expressed as

$$Q_i = C_i(p_{i,res} - p_i) \tag{1}$$

where p_i is the pressure in the small basin at the height of tube i, $p_{i,res}$ is the pressure in the reservoir at that height and C_i is the hydraulic resistance of tube i. Note that flow into the small basin is defined positive. The pressures in the small basin and the reservoir are assumed to be hydrostatic, and furthermore a linear equation of state is used

$$\rho = \rho_0(1 - \alpha(T - T_0) + \beta S) \tag{2}$$

where ρ_0 is the density of fresh water at room temperature. The pressures in the reservoir are then given by

$$p_{1,res} = 0 \tag{3a}$$
$$p_{2,res} = \rho_0 g D/2 \tag{3b}$$
$$p_{3,res} = \rho_0 g(D - d) + \rho_0 g(1 + \beta S_0)d \tag{3c}$$

Using the Boussinesq approximation by assuming that βS, βS_0 and $|\alpha T| \ll 1$ everywhere, the pressures p_1, p_2 and p_3 in the small basin are

$$p_1 = \rho_0 g\eta \tag{4a}$$
$$p_2 = \rho_0 g\eta + \rho_0 g D/2 + \rho_0 g(\delta - D/2)(\beta S - \alpha T) \tag{4b}$$
$$p_3 = \rho_0 g\eta + \rho_0 g D + \rho_0 g\delta(\beta S + \alpha T) \tag{4c}$$

where η is the surface elevation in the small basin with respect to the water surface in the reservoir and δ is the distance of the layer of convecting fluid in the small basin above the second tube. The volume fluxes are then given by

$$Q_1 = -C\rho_0 g \quad \eta \tag{5a}$$
$$Q_2 = C\rho_0 g \quad [-\eta + (\delta - D/2)(\alpha T - \beta S)] \tag{5b}$$
$$Q_3 = \gamma C\rho_0 g \quad [-\eta + \beta S_0 d + \delta(\alpha T - \beta S)] \tag{5c}$$

Following Whitehead [4], we assume that the hydraulic resistance of the upper two tubes is equal to C and that the resistance of the bottom tube is $C_3 = \gamma C$, with γ a positive number.

If the heating is so weak that the interface between the convecting and the non-convecting layer in the small basin is below the middle tube, steady state solutions are not possible, because mass cannot be conserved. For larger heating rates the interface will be between the middle and the upper tube, so that $\delta < D$. In this case steady state solutions can occur, but only if there is no flow through the upper tube, again because otherwise mass would not be conserved, so we have $Q_1 = 0$ and $\eta = 0$. The equation for steady state mass conservation reduces in this case to $Q_2 + Q_3 = 0$. Together with equation (5) this gives that the depth of the convecting layer is

$$\delta = \frac{1}{1+\gamma}\left[\frac{D}{2} - \frac{\gamma\beta S_0 d}{\alpha T - \beta S}\right] \tag{6}$$

yielding for the volume fluxes

$$Q_1 = 0 \tag{7a}$$
$$Q_2 = \frac{\gamma C\rho_0 g[(\beta S - \alpha T)D - 2\beta S_0 d]}{2\gamma + 2} \tag{7b}$$
$$Q_3 = -\frac{\gamma C\rho_0 g[(\beta S - \alpha T)D - 2\beta S_0 d]}{2\gamma + 2} \tag{7c}$$

It can easily be shown that the case in which $Q_2 > 0$ and $Q_3 < 0$ is inconsistent, so we have to have inflow through the bottom tube and outflow through the middle tube ($Q_2 < 0$ and $Q_3 > 0$) as long as the interface in the small basin is between the top and middle tube. In this case the steady state heat budget is

$$0 = H + \rho_0 C_p Q_2 (T + T_0) + \rho_0 C_p Q_3 T_0 \tag{8}$$

where H is the heat flux into the small basin due to the heating at the bottom and C_p is the specific heat capacity. The steady state salt budget is

$$0 = Q_2 S + Q_3 S_0 \tag{9}$$

Using mass conservation, the steady state heat and salt budgets can be rewritten as

$$H = \rho_0 C_p Q_3 T; \quad S = S_0 \tag{10}$$

As we are considering the case for which $Q_2 < 0$, this gives that the temperature in the small basin has to be higher than a certain critical value T_{nil} in order to have steady state solutions, with

$$T_{nil} = \frac{\beta S_0}{\alpha}\left(1 - \frac{2d}{D}\right) \tag{11}$$

If the heating rate H is increased, the temperature and the height of the convecting layer will also increase. For a certain heating rate, the interface between the convecting and the non-convecting water will reach the upper tube. The critical temperature T_c at which this happens follows from $\delta = D$ and is given by

$$T_c = \frac{\beta S_0}{\alpha}\left(1 - \frac{2\gamma d}{(1+2\gamma)D}\right) \tag{12}$$

For $T > T_c$ there is also flow in the upper layer and the equation for mass conservation becomes

$$Q_1 + Q_2 + Q_3 = 0 \tag{13}$$

The interface stays at height D for temperatures greater than T_c as we have used the Boussinesq approximation. The height of the interface follows therefore from equations (5) and (13) with $\delta = D$ as

$$\eta = \frac{2\gamma\beta S_0 d + (\alpha T - \beta S)D(2\gamma+1)}{2(2+\gamma)} \tag{14}$$

so that the volume fluxes become

$$Q_1 = \frac{C\rho_0 g}{2+\gamma}\left[-\frac{1+2\gamma}{2}(\alpha T - \beta S)D - \gamma\beta S_0 d\right] \tag{15a}$$

$$Q_2 = \frac{C\rho_0 g}{2+\gamma}\left[-\frac{\gamma-1}{2}(\alpha T - \beta S)D - \gamma\beta S_0 d\right] \tag{15b}$$

$$Q_3 = \frac{\gamma C\rho_0 g}{2+\gamma}\left[\frac{3}{2}(\alpha T - \beta S)D + 2\beta S_0 d\right] \tag{15c}$$

which is consistent with equation (5) for $T = T_c$ and $\delta = D$.

At the critical temperature T_c we have $S = S_0$ and thus $Q_1 = 0$, $Q_2 < 0$ and $Q_3 > 0$. The positive surface elevation in the small basin causes the pressure at the height of the upper tube in the small basin to be higher than that in the reservoir, giving flow out of the small basin. From equations (12) and (14) we can see that if $T > T_c$ we will always have $\eta > 0$, which says that in order to have flow in the upper tube, the surface elevation has to be positive. So the flow in the upper tube will either be zero if the interface is below the upper tube or positive if the interface is at the top of the small basin. At mid-depth, the effect of salinity on the density dominates over the effect of temperature, so that at mid-depth there is a higher pressure in the small basin than in the reservoir. At the bottom however, the pressure in the reservoir is higher than that in the small basin, because the water in the reservoir is much colder than that in the small basin.

From equation (15) we see that for $T > T_c$ Q_1 becomes negative starting from zero and Q_3, which is already positive, becomes more positive, also if $S \neq S_0$ (note that S can never

become greater than S_0). For $\gamma \geq 1$ Q_2, which is negative already, becomes more negative, so that no fresh water can enter the small basin and the small basin stays always filled with water of salinity S_0. If $\gamma < 1$ however, Q_2, which is negative, becomes less so and eventually will become zero. So if the resistance of the bottom tube is higher than those of the middle and upper tubes, there is a value of the heating rate for which the flow in the second tube reverses sign, so that fresh water can enter the small basin. Note though that there will always be inflow through the bottom tube and outflow through the top tube.

The point for which $Q_2 = 0$ defines a second critical temperature

$$T_{cc} = -\frac{\beta S_0}{\alpha}\left[\frac{2\gamma d}{(\gamma-1)D} - 1\right] \tag{16}$$

At this temperature the water is heated so much, that the effect of the temperature dominates over the effect of salinity and the pressure due to the surface elevation. The pressure in the small basin at mid-depth is now lower than the pressure in the reservoir at that height and there will be inflow of cold and fresh water into the small basin. For $T_c < T < T_{cc}$ the heat and salt balances are still given by equation (10). For $T > T_{cc}$ the steady state heat and salt balances are

$$0 = H + \rho_0 C_p Q_1 T \tag{17a}$$

$$0 = Q_1 S + Q_3 S_0 \tag{17b}$$

As the solutions of equations (15) and (17) are complicated polynomials, we calculate them numerically, using time-dependent heat and salt balances. The equations are made dimensionless using

$$\tilde{Q} = \frac{Q}{Q_s}, \quad Q_s = \frac{\gamma C \rho_0 g \beta S_0 D}{2+\gamma}, \quad \tilde{T} = \frac{\alpha T}{\beta S_0}, \quad \tilde{d} = \frac{d}{D}, \quad \tilde{S} = \frac{S}{S_0} \tag{18a}$$

$$\tilde{t} = \frac{t}{AD/Q_s}, \quad \tilde{H} = \frac{H}{\rho_0 c_p T_s Q_s}, \quad T_s = \frac{\beta S_0}{\alpha} \tag{18b}$$

where Q_s is the volume flux scale, t is time and A is the horizontal area of the small basin. The dimensionless form of equation (7) is

$$\tilde{Q}_2 = -\tilde{Q}_3 = \frac{2+\gamma}{2+2\gamma}\left(1 - \tilde{T} - 2\tilde{d}\right) \tag{19}$$

and equation (15) transforms to

$$\tilde{Q}_1 = \quad -\tfrac{2+1/\gamma}{2}(\tilde{T} - \tilde{S}) - \tilde{d} \tag{20a}$$

$$\tilde{Q}_2 = \quad -\tfrac{1-1/\gamma}{2}(\tilde{T} - \tilde{S}) - \tilde{d} \tag{20b}$$

$$\tilde{Q}_3 = \quad \tfrac{3}{2}(\tilde{T} - \tilde{S}) + 2\tilde{d} \tag{20c}$$

The dimensionless time-dependent heat and salt balances are

$$\frac{d\tilde{T}}{dt} = \tilde{H} + \tilde{T}[\tilde{Q}_1\Gamma(-\tilde{Q}_1) + \tilde{Q}_2\Gamma(-\tilde{Q}_2) + \tilde{Q}_3\Gamma(-\tilde{Q}_3)] \tag{21}$$

$$\frac{d\tilde{S}}{dt} = \tilde{Q}_1\tilde{S}\Gamma(-\tilde{Q}_1) + \tilde{Q}_2\tilde{S}\Gamma(-\tilde{Q}_2) + \tilde{Q}_3[\tilde{S}\Gamma(-\tilde{Q}_3) + \Gamma(\tilde{Q}_3)] \tag{22}$$

Numerical solutions were calculated for a wide range of heating rates by integrating equations (21) and (22), using (19) and (20), until a steady state was reached. If the heating rate depends on the temperature in the small basin via

$$\tilde{H} = K(\tilde{T}^* - \tilde{T}) \tag{23}$$

with K a constant, then Whitehead [4] shows that in the equivalent system for the Arctic-Ocean case multiple equilibria can be found: both shallow and deep convection states can exist for the same forcing temperature. The range of forcing temperatures $\tilde{T}^*$ for which multiple equilibria occur, depends on the parameters $\tilde{d}$, γ and K. A typical plot of temperature and salinity in the small basin as a function of forcing temperature for our case (heating from below) is shown in Fig. 2. The shallow convection states have a relatively

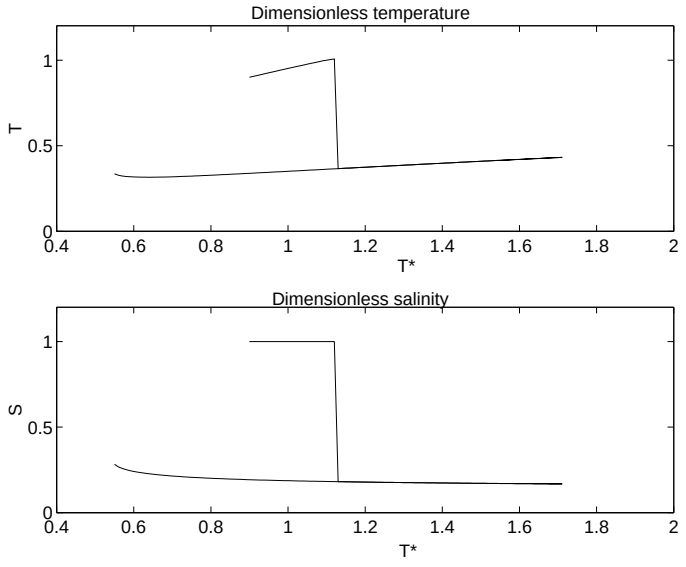

Figure 2: Dimensionless temperature and salinity as a function of (dimensionless) forcing temperature $\tilde{T}^*$ for the case with $\gamma = 0.05$, $d = 0.05$ and $K = 1$.

high temperature, and a dimensionless salinity $\tilde{S} = 1$, as only the salty water can enter the small basin. If T^* is increased above $\tilde{T}_{cc}$, deep convection states occur, with inflow of fresh and relatively cold water through the middle tube. In the deep convection states the temperature and the salinity are therefore much lower. If the forcing temperature is then decreased slowly, the system will remain in the deep convection state.

3 Experiments

3.1 Apparatus and method

The laboratory model consisted of a box of $20 \times 20 \times 20$ *cm* (the reservoir) that was connected via three tubes to a cylindrical small basin of 20 *cm* high with a diameter of about 5 *cm* (Fig.

3). The vertical distance between the centers of the top and bottom tubes was $D = 18\ cm$. The top, middle and bottom tubes had lengths of 99 mm, 98 mm and 9 mm, respectively.

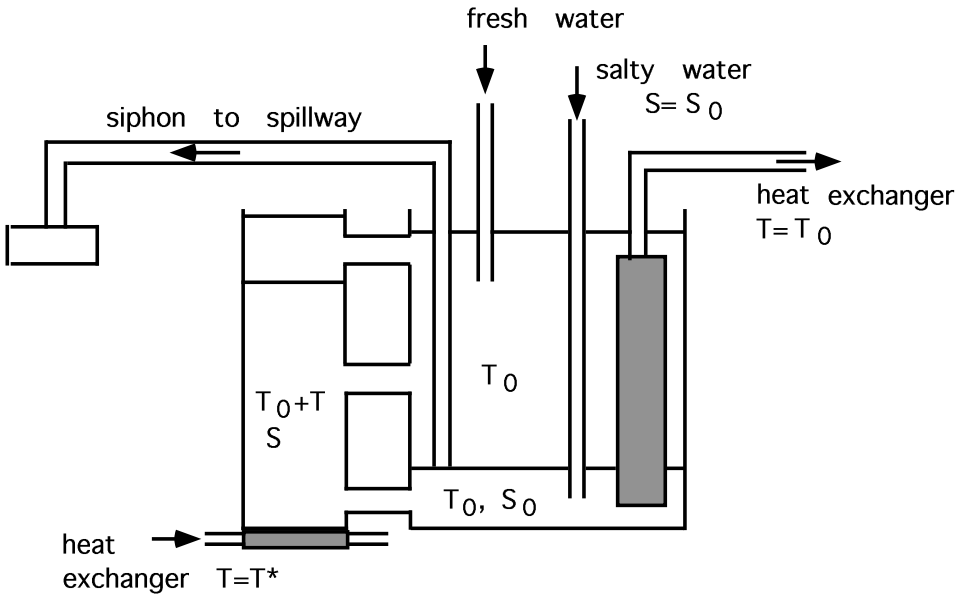

Figure 3: Sketch of the laboratory model (vertical section). The small basin is heated from below by a heat exchanger. Both fresh and salty water are pumped in at the top and bottom, respectively, and removed by a siphon at a fixed depth, thus maintaining a sharp interface between the salty and the fresh layer. A second heat exchanger keeps both layers in the reservoir at room temperature.

Fresh water at room temperature (about $21 \pm 2°C$) was pumped into the top of the reservoir at a rate of about 0.1 l/min, and salt water of the same temperature was pumped into the bottom of the reservoir at the same rate. The sum of these two fluxes was removed by a siphon that was placed at a certain distance above the center of the bottom tube. This maintained a sharp interface between the fresh and the salty water, at a level determined by the height of the siphon. The salty water was made by mixing fresh and salt water and adjusting this mixture to obtain a density of 1003.4 kgm^{-3} at room temperature, so that the density difference between the two layers in the reservoir was 5.2 kgm^{-3}. The salty water was dyed blue to see the difference between salty and fresh water. A heat exchanger flushed by water of $20°C$ was placed in the reservoir along the side opposite to the tubes. The reservoir was monitored routinely and both layers remained at $20°C$ within a range of $\pm 1.3°C$. The bottom of the small basin was heated by a second heat exchanger, which was flushed by water of a desired temperature.

Experiments have been done for two configurations. In the main experiments the radii of the top, middle and bottom tubes had their standard values $r_1 = r_2 = 9.5\ mm$ and $r_3 = 1.5\ mm$, respectively and the siphon was placed at $d = 0.6\ cm$ above the center of the bottom tube. In the second set of experiments the upper and the middle tube had radii $r_1 = 4.5\ mm$ and $r_2 = 3.1\ mm$, respectively (the radius of the bottom tube was still 1.5 mm), and the siphon was at 1.4 cm above the center of the bottom tube. The parameter

Set 1				Set 2			
d	=	0.6	cm	d	=	1.4	cm
r_1	=	9.5	mm	r_1	=	4.5	mm
r_2	=	9.5	mm	r_2	=	3.1	mm
r_3	=	1.5	mm	r_3	=	1.5	mm

Table 1: Values of parameters used in the two sets of experiments. The parameters of set 1 are the standard values.

values for the two sets of experiments are summarized in Table 1.

The temperature in the small basin was measured with three digital thermometers, with probes at 0.5 cm, 8.5 cm and 17.5 cm above the bottom. In some experiments, two additional temperature probes, which were connected to dataloggers, were placed at about 2 cm and 8 cm above the bottom. The dataloggers recorded the temperature once every 15 s. The experiments were also recorded on video tape. After a steady state had been reached, samples were taken near the bottom, in the middle and just below the top of the water column. With a densiometer the density of these samples could be measured. The salinity of the sample can then be determined from this density (which is measured at room temperature) and the density of fresh water at room temperature.

An experiment was started by filling both basins with fresh water, after which the salt water pump was switched on at a high flow rate. Within less than fifteen minutes the salty layer in the reservoir had formed. Then the fresh and salt water pumps were set at their normal rates and the temperature of the heat exchanger at the bottom of the small basin was set at the desired value. Then the system was left to come to equilibrium. This took typically two or three hours for the experiments of the first set, and six or more hours for the experiments of the second set.

Test measurements were done for different forcing temperatures. As water can contain less dissolved gases when it is heated, air bubbles will form on the bottom and the side walls of the small basin, and in particular around the opening of the bottom tube during an experiment. It turned out that, if the forcing temperature was about $35°C$ or higher, the flow through the bottom tube would get blocked by air bubbles in typically one or two hours. A situation in which this happened could be recognized visually by the fact that the water in the small basin became completely colorless. A sample taken from this water showed that the density was equal to that of fresh water. This is consistent with a blocked bottom tube, as salty water can then no longer enter the small basin.

The use of distilled fresh water in combination with de-aerated salt water did not solve the problem. Therefore we partly de-aerated the water of the salty mixture, by heating the water up to a temperature of about $45°C$ to $50°C$ and keeping it at this temperature for several hours. Then the water was left for one or two days to cool down to room temperature again. However, even with this procedure it remained necessary to remove the air bubbles regularly, by sticking a small metal wire into the bottom tube. This could be done with hardly any disturbance of the flow. Usually we removed air bubbles in this way about once every 30 minutes.

3.2 Convective oscillations

The forcing temperature T^* was varied between $35°C$ and $50°C$ for standard values of the parameters (Table 1). Two different flow regimes were found: for forcing temperatures $T^* = 42°$ and higher, the system reached a steady state within one or two hours, whereas self-sustained oscillations occurred for lower forcing temperatures. The temperature and the salinity contribution to the density in the small basin near the bottom and at mid-depth are plotted against the forcing temperature T^* in Fig. 4 for both steady states and oscillations.

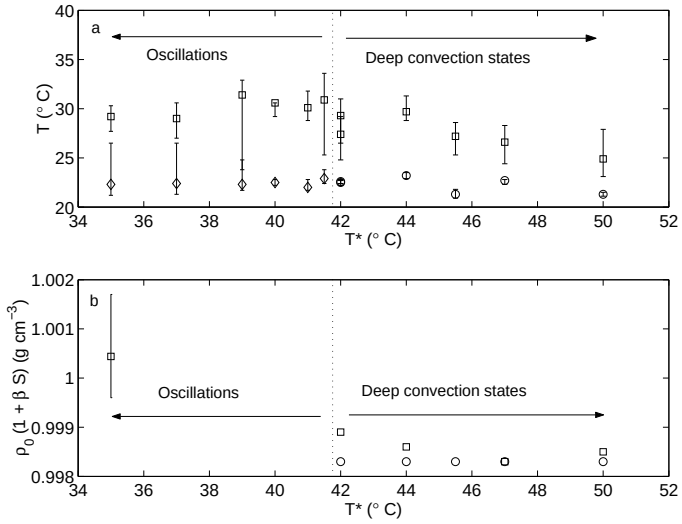

Figure 4: (a) Average temperature in the small basin as a function of the forcing temperature T^*. (b) Salinity contribution to the density (a measure for the salinity) in the small basin as a function of T^*. The squares are values at the bottom, the circles and diamonds are values at mid-depth. Temperature and salinity at the top are not plotted, as they were almost equal to the values at mid-depth. Average temperatures were calculated by averaging the temperature at 5 minute-intervals over one hour, or, in the case of oscillations with periods greater than one hour, by averaging temperatures at 15-minute intervals over one oscillation period. Vertical bars indicate the minimum and maximum values.

The average temperature at mid-depth lies around $22°C$ or $23°C$ for both the steady states and the oscillations, whereas the temperature at the bottom is several degrees higher. This is because the bottom temperature is measured within the thermal boundary layer that exists in a convecting fluid, heated from below [5], whereas the mid-depth temperature is measured in the well-mixed region. Temperatures at the top of the small basin are almost the same as at mid-depth and are therefore not shown. In all steady states there is flow into the small basin through the bottom and middle tube and outflow through the upper tube, which characterizes these states as deep convection states. In the steady states, the water in the small basin also has a very low salinity (Fig. 5b), due to the relatively strong inflow of fresh water through the middle tube (the diameter of the middle tube is much bigger than that of the bottom tube). The temperatures at mid-depth and near the bottom of the small basin as a function of time for a typical oscillation are shown in Fig. 5.

We start the description at the arbitrarily chosen time $t = 2.5\ hr$, when a layer of salty water has started to form at the bottom of the small basin. This could clearly be seen as a small layer of blue water at the bottom. The bottom temperature is at its maximum, whereas the temperature at mid-depth is low. As time progresses, the salty, convecting layer grows (during about one hour). The bottom temperature decreases only slightly, until the interface between the warm, salty water and the colder, fresher water breaks up rather rapidly and the whole water column mixes in typically several minutes (at $t = 3.2\ hr$ in Fig. 5). At this moment, the bottom temperature decreases rapidly, as the water at the bottom mixes with the colder water from the layer above. At the same time the temperature in the middle of the basin increases suddenly, due to the mixing with the much warmer water from the bottom layer. Then the whole water column is well mixed, which could be seen in the experiment because the whole water column was colored light blue. Within about ten minutes, during which the bottom temperature remains low, the water in the small basin becomes almost fresh (around $t = 3.4\ hr$). Then the cycle repeats itself. During the whole oscillation there was inflow through the middle tube and outflow through the top tube.

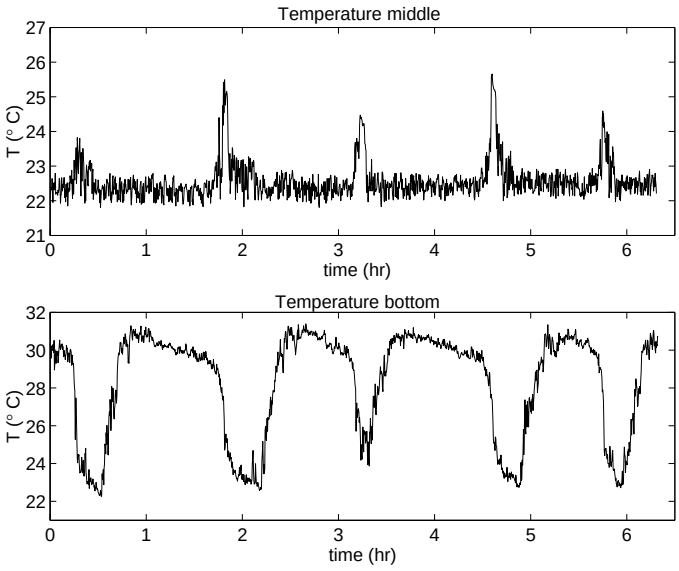

Figure 5: Temperature (a) at mid-depth and (b) at the bottom of the small basin as a function of time for the experiment with $T^* = 39°$.

During the experiment with $T^* = 35°C$, the salinity was measured at several times during an oscillation cycle (Fig. 6). While the convecting layer of salty water is growing and the temperature near the bottom is relatively high (Fig. 6a, between about 1 hr and 4.5 hr), the salinity decreases rapidly (Fig. 6b), due to entrainment of fresh water from the layer above. The salinity increases again when a new layer of salty water starts to form.

The oscillation mechanism can be understood by considering the vertical density profiles. At a certain point during the oscillation the whole water column is well mixed, so that the density is constant with depth. However, the inflow of salty water through the bottom tube creates a salty layer at the bottom of the small basin. Because the water is also heated from below, a well mixed salty layer will form at the bottom. This layer is heavier than the

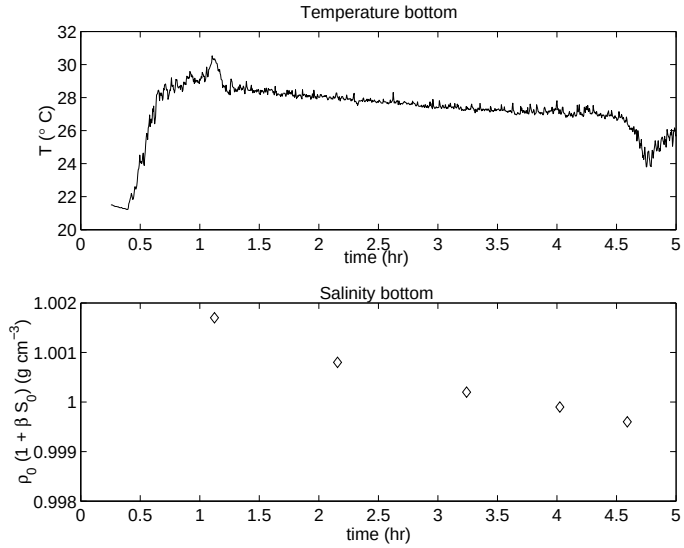

Figure 6: (a) Temperature at the bottom of the small basin as a function of time for the experiment with $T^* = 35°$. (b) Salinity contribution to the density at the bottom of the small basin as a function of time for the experiment with $T^* = 35°$.

fresher water above it due to its high salinity, so that the density profile will show a stable density step. The inflow of salty water and the entrainment of fresher water from the layer above make the salty layer grow in time, but the entrainment also decreases the salinity. As the temperature of this layer does not change very much, the density of the lower layer decreases. The temperature of the upper layer will increase slightly due to conduction of heat across the interface, but this is only a small effect. Finally, the effects of temperature and salinity on the density in the lower layer compensate so that both layers have equal density. On a slight decrease in salinity of the lower layer the water column now becomes unstable, causing the whole water column to overturn. The inflow of cold, fresh water through the middle tube and the outflow of well-mixed water through the top tube will lower the salinity and temperature and then the whole cycle starts again.

The period of the oscillation decreases with increasing forcing temperature (Fig. 7a), as stronger convection in the salty layer causes more entrainment and therefore a faster decrease of the density difference between the two layers, and correspondingly a shorter period. The maximum height of the salty layer during the oscillation also decreases with increasing forcing temperature (Fig. 7b). At higher forcing temperatures, the density difference decreases faster, so that the salty layer has not yet become very big when the water column overturns already.

3.3 Other flow regimes

In the second set of experiments, in which the upper and middle tubes had smaller diameters (Table 1), the forcing temperature was varied between $37°C$ and $46°C$ (Fig. 8). For all forcing temperatures within this range, the system eventually reached a steady state.

For forcing temperatures of $44°C$ and lower shallow convection states were found, with

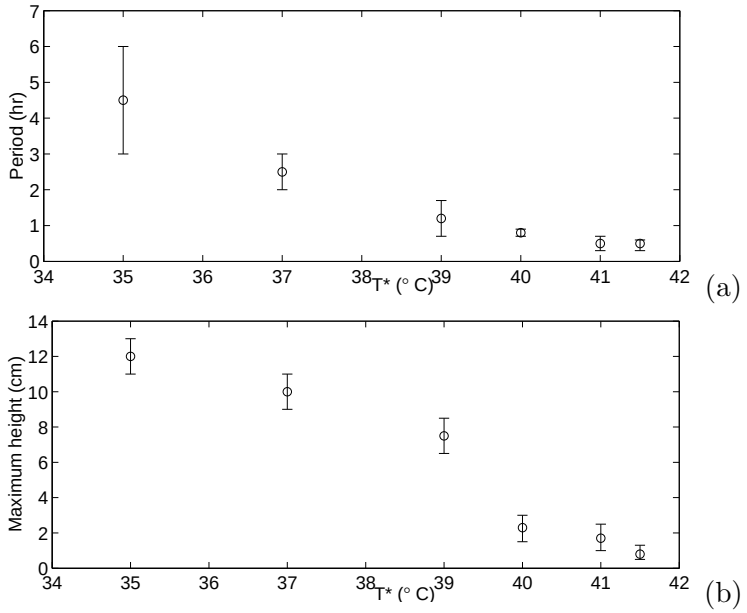

Figure 7: (a) Period of the oscillation as a function of forcing temperature T^*. (b) Maximum height of the salty layer during the oscillation as a function of T^*. The vertical bars indicate the range of maximum and minimum values of the period and the layer height, respectively.

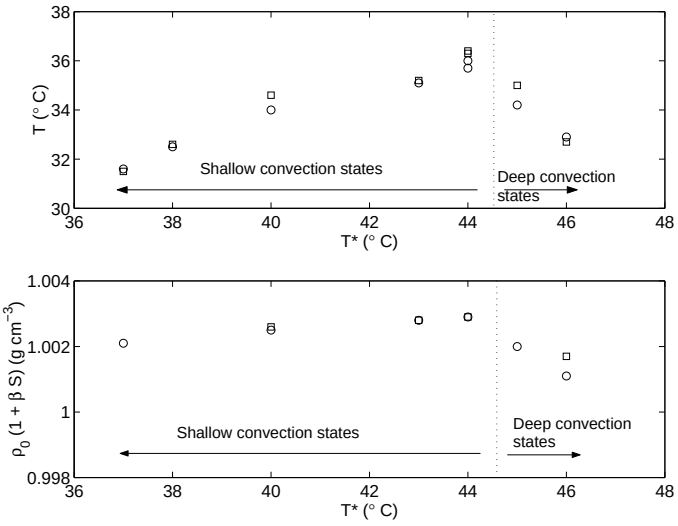

Figure 8: (a) Average temperature in the small basin as a function of the forcing temperature T^*. (b) Salinity contribution to the density in the small basin as a function of T^*. Squares indicate values at the bottom, circles values at mid-depth. Average temperatures were calculated by averaging the temperature at about 15 minute-intervals over one or two hours.

inflow through the bottom tube and outflow through the middle and top tubes. Deep convection states, with inflow through the bottom and middle tubes and outflow through the top tube, existed for forcing temperatures of $45°C$ and $46°C$. The temperatures at mid-depth and near the bottom of the small basin are almost the same (Fig. 8a), indicating that the thermal boundary layer is smaller than in the first set of experiments, so that bottom temperatures are now measured within the well-mixed layer. In the shallow convection states, the temperature in the small basin increases from about $31.5°C$ at $T^* = 37°C$ to about $36°C$ at $T^* = 44°C$. In the deep convection states, temperatures are lower again, due the inflow of relatively cold water through the middle tube. The salinity is relatively high in the shallow convection states (Fig. 8b) and is lower in the deep convection states, because the inflow through the middle tube is also fresh.

The two types of steady states could easily be distinguished, as in the shallow state the water in the small basin was blue (salty), whereas it was almost colorless (almost fresh) in the deep convection state. Also, the middle tube contained blue water in the shallow convection states (as there is outflow through that tube in a shallow convection state) and colorless water in a deep convection state (inflow through the middle tube). The flow in the middle and top tubes could also be visualized by injecting a little bit of red dye at one end of the tube.

Unfortunately, as the time needed to reach equilibrium was often more than six hours and as the air bubbles had to be removed regularly to prevent the bottom tube from being blocked, it was not possible to change the forcing temperature slightly after an equilibrium had been reached and let the system come to equilibrium again. Therefore, we could not investigate the possibility of multiple equilibria.

4 Comparison with theory

The experimental results can be compared to the box model theory, if the values of the model parameters γ, K and $\tilde{d}$ are known. These parameters have been determined for the first set of experiments (the standard configuration). The parameter $\tilde{d}$ is given by the distance between the height of the siphon inlet and the center of the bottom tube divided by the total height of the water column and was $\tilde{d} = 0.033$. The values of γ and K can be determined indirectly from measurements.

The ratio γ of the hydraulic resistances of the bottom and middle tube (the top and middle tubes are equal) depends on the characteristic flow timescales τ_b and τ_m of the bottom and middle tube, respectively. These two timescales can be determined as follows. Consider first the situation in which the small basin is filled with a layer of salty water of initial thickness h_0 (with $h_0 > d$) at the bottom and fresh water above it. Furthermore the middle tube is blocked, so that salty water will flow out of the small basin through the bottom tube (and fresh water will enter through the top tube). If the thickness of the salty layer in the small basin is denoted by $h(t)$, then the time evolution of h is given by

$$A\frac{dh}{dt} = Q_3 \tag{24}$$

where A is the horizontal area of the small basin. The flow rate Q_3 can be determined from

the pressure difference between both ends of the bottom tube and is given by

$$Q_3 = \gamma C \rho_0 g[-\eta + \beta S_0(d-h)] \tag{25}$$

If changes in surface elevation with time can be neglected, we can use $Q_1 + Q_3 = 0$, which gives

$$Q_3 = \frac{\gamma C \rho_0 g \beta S_0 (d-h)}{(1+\gamma)} \tag{26}$$

Then equation (24) turns into

$$\frac{dh}{dt} = -\frac{1}{\tau_b}(h-d) \tag{27}$$

with solution

$$h(t) = (h_0 - d)e^{-t/\tau_b} + d \tag{28}$$

where the constant τ_b is the characteristic timescale associated with flow in the bottom tube, given by

$$\tau_b = \frac{A(1+\gamma)}{C\rho_0 g \gamma \beta S_0} \tag{29}$$

An estimate of the time constant τ_m of the middle tube can be obtained when the same experiment is done, but now with the bottom tube instead of the middle tube blocked. The equation for the evolution of the layer thickness h', defined as the height of the layer of salty water above the center of the middle tube, is

$$\frac{dh'}{dt} = -\frac{h'}{\tau_m} \tag{30}$$

where

$$\tau_m = \frac{2A}{C\rho_0 g \beta S_0} \tag{31}$$

This has solution

$$h' = h'_0 e^{-t/\tau_m} \tag{32}$$

with h'_0 the initial layer thickness. From equations (29) and (31) it can easily be seen that

$$\gamma = \frac{\tau_m}{2\tau_b - \tau_m} \tag{33}$$

The constants τ_b and τ_m were determined by measuring h and h' as a function of time and fitting exponential curves to the data points. We found $\tau_b = 1080 \pm 10\ s$ and $\tau_m = 9 \pm 2\ s$, which gives $\gamma = 0.004 \pm 0.001$.

Another experiment was done to determine K. Consider the dimensional form of equation (23), which is

$$H = K^*(T^* - T) \tag{34}$$

where the dimensional heat exchange coefficient K^* is related to K via $K^* = \rho_0 C_p Q_s K$. If a layer of area A and thickness D is heated, then equation (34) can be written as

$$\frac{dT}{dt} = \frac{1}{\tau_T}(T^* - T) \tag{35}$$

where the thermal relaxation timescale τ_T is given by

$$\tau_T = AD/(Q_s K) \tag{36}$$

This has solution

$$T(t) = (T_0 - T^*)e^{-t/\tau_T} + T^* \tag{37}$$

The volume flux scale Q_s in (36) follows from (18a) and (29) and is

$$Q_s = \frac{AD}{\tau_b}\frac{1+\gamma}{2+\gamma} \tag{38}$$

Equations (36) and (38) can now be combined to yield

$$K = \frac{\tau_b}{\tau_T}\frac{2+\gamma}{1+\gamma} \tag{39}$$

The thermal time constant τ_T was measured by heating a layer of 19 cm of fresh water with $T^* = 41°C$. This gave $\tau_T = 2800 \pm 300$ s. When a layer of salty water of 9.5 cm (with fresh water above it) was heated with $T^* = 41°C$, a value $\tau_T = 1680 \pm 360$ s was obtained. These estimates of τ_T yielded values of K between $K = 0.6$ and $K = 1.7$. For our calculations we chose therefore $K = 1.2 \pm 0.5$.

The temperature and salinity data are non-dimensionalized using $\tilde{T} = \alpha T/\beta S_0$ and $\tilde{S} = S/S_0$ as in (18), with $\alpha = 3 \cdot 10^{-4}$ K^{-1} and $\beta S_0 = 5.2 \cdot 10^{-3}$, and compared to the theoretical curves for $\gamma = 0.004$, $K = 1.2$ and $\tilde{d} = 0.033$ (Fig. 9). The temperature and

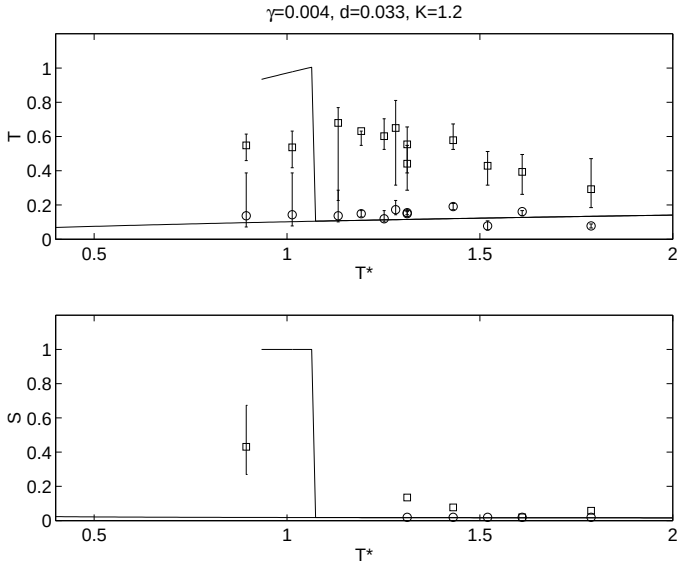

Figure 9: (a) Dimensionless temperature as a function of the dimensionless forcing temperature $\tilde{T}^*$. (b) Dimensionless salinity as a function of $\tilde{T}^*$. Solid lines are the theoretical curves, squares are measurements at the bottom and circles are measurements at mid-depth. Vertical bars indicate the maximum and minimum values of the measurements.

salinity at mid-depth for the deep convection states ($\tilde{T}^* \geq 1.3$) agree quite well with the

theoretical curve for the deep convection states. As was mentioned before, the bottom temperatures are much higher, as these are measured in the thermal boundary layer and do not represent the temperature of the well mixed layer, as the theoretical curves do. The average mid-depth temperatures for the oscillations ($\tilde{T}^* < 1.3$) agree also rather well with the theoretical curve for the deep convection steady states, but the reason for that is not yet clear.

5 Discussion and conclusions

A laboratory experiment has been conducted in which a small basin, that was connected to a large reservoir via three tubes, was heated from below. The reservoir had a shallow layer of salty water underneath a much bigger layer of fresh water, and both layers were kept at room temperature. It was shown that different flow regimes exist in this laboratory experiment.

An oscillatory regime exists for forcing temperatures below $42°C$, whereas there is a regime of steady deep convection states for higher forcing temperatures. The deep convection states are characterized by inflow of cold and salty water through the bottom tube into the small basin, inflow of cold and fresh water through the middle tube and outflow through the top tube. These deep convection states are in good agreement, both qualitatively and quantitatively, with the box model theory developed by Whitehead [4].

During an oscillation a convecting layer of salty water grows and entrains fresh water, thereby decreasing its density, until the water column becomes unstable and convection extends through the whole water column. The oscillation period decreases with increasing forcing temperature, as for a higher forcing temperature an unstable stratification is reached quicker, because there is more entrainment of fresh water. The box model theory presented in section 2 cannot explain this oscillation, even if time-dependent heat and salt balances are considered as in equation (21) and (22), because this theory does not take into account processes like entrainment and mixing of the two layers, which are crucial for the oscillation mechanism. A more quantitative theory for these oscillations still has to be developed.

It is helpful to return to the oceanic case for a moment and consider what this oscillation might look like in a situation where the small basin is cooled from above and connected to a reservoir with a shallow layer of fresh water overlying salty water. The inflow of fresh water through the upper tube will then create a surface layer of fresh water, that is convecting and extending downward as it is cooled from above. This layer will entrain salty water from below until it is dense enough to cause the whole water column to overturn. If the inflow of fresh water at the top is strong enough, deep convection stops and the cycle starts again. It is interesting to note that in this oscillation the fresh surface layer has to become saltier before deep convection can occur, similar to the fact that surface waters in the polar ocean are very fresh and have to become locally saltier before a deep convection event can happen. Although it is not straightforward to apply the results from such a laboratory model to the real ocean, these results suggest that deep convection in the ocean might be related to an internal oscillation, with deep convection occurring only during relatively short intervals.

It is not yet clear what role double diffusive processes play in this experiment. During the slow phase of the oscillation there is cold, fresh water overlying warm and salty water, which corresponds to the 'diffusive' regime in double diffusive problems. However, the

oscillation we find is different from the oscillatory instability in this diffusive regime [5], as we are certainly in the turbulent regime.

In a configuration in which the upper and middle tubes have smaller diameters (but still larger than that of the bottom tube), no oscillations were found. Instead, a regime of shallow convection states exists for forcing temperatures below $45°C$, in which there is inflow through the bottom tube and outflow through the middle and top tubes. For high forcing temperatures (above $45°C$), deep convection states were found.

It is still unclear why oscillations do not occur in this second set of experiments. This must have to do with the different flow rates and therefore also the different temperatures and salinities in the small basin, due to the different tube diameters. Unfortunately, τ_m has not been measured for the second set of experiments, so that the results from Fig. 8 cannot be compared with the theory. Another unanswered question is why steady shallow convection states were not found in the standard configuration, although the box model theory (that seems to work very well for higher forcing temperatures) predicts their existence between $\tilde{T}^* = 0.9$ and $\tilde{T}^* = 1.1$. Either shallow convection states cannot occur here, because oscillations prevent the establishment of a steady state, or steady shallow convection states do exist, but for much lower forcing temperatures. Further study is required to understand under what conditions the different flow regimes occur.

In future work also a new apparatus might be devised, to make the experiments faster. The flow through the bottom tube should also no longer get blocked by air bubbles. Then the question whether or not this laboratory experiment can also exhibit multiple equilibria can be investigated.

Acknowledgments

I would like to thank Jack Whitehead for his very enthusiastic support and supervision of this project. Special thanks also to Keith Bradley, who had many practical suggestions and also created a real nice atmosphere in the lab. Discussions with Joe Keller and George Veronis were both very pleasant and very useful. Finally, I would like to thank all the fellows for their friendship and support during this enjoyable summer.

References

[1] P. D. Killworth, "Deep convection in the world ocean," Rev. Geophys. Space Phys. **21**, 1 (1983).

[2] H. U. Sverdrup, M. W. Johnson, and R. H. Fleming, *The Oceans. Their physics, chemistry and general biology* (Prentice-Hall, New York, 1942).

[3] M. Tomczak and J. S. Godfrey, *Regional Oceanography: an introduction* (Pergamon, New York, 1994).

[4] J. A. Whitehead, "Stratified convection with multiple states," Ocean Modelling **2**, 109 (2000).

[5] J. S. Turner, *Buoyancy effects in fluids* (University press, Cambridge, 1973).